Influence of Organic Liquids on the Nanostructure of Precipitated Cellulose

Brian J. Watson,[1,2] Boualem Hammouda,[3] Robert M. Briber,[1] Steven W. Hutcheson[2]

[1]Department of Materials Science and Engineering, University of Maryland, College Park, Maryland 20742
[2]Department of Cell Biology and Molecular Genetics, University of Maryland, College Park, Maryland 20742
[3]National Institute of Standards and Technology, Center for Neutron Research, Gaithersburg, Maryland 20899
Correspondence to: S. W. Hutcheson (E-mail: hutcheso@umd.edu)

ABSTRACT: Organic liquids have been used in pretreatments to improve the digestibility of lignocellulosic biomass, ultimately reducing the amount of enzyme required to digest the material to its constituent sugars. To understand the influence of these solvents on cellulose nanostructure, phosphoric acid was used to solubilize cellulose (PAS cellulose) followed by washing of the PAS cellulose with organic liquids previously demonstrated to aid pretreatment. PAS cellulose washed using methanol, ethanol, and ethylene glycol had gel-like properties with disrupted nanostructures. PAS cellulose washed with acetone, 2-propanol, and water yielded an opaque white precipitate. Small-angle neutron scattering indicated the formation of loosely bundled rods of cellulose in the gel-like material. Fourier transform infrared resonance of solvent-washed, flash-dried PAS cellulose suggested an increase in interchain hydrogen bonds in the gel-like precipitates relative to the more obvious precipitates formed in other solvents. The optimal wash liquid was determined to be 40% by volume ethanol in water to induce a highly digestible, gel-like material. © 2012 Wiley Periodicals, Inc. J. Appl. Polym. Sci. 000: 000–000, 2012

INTRODUCTION

Polymeric cellulose (β-1,4 glucan) is a major component of lignocellulosic biomass.[1,2] During synthesis of the plant cell wall, cellulose polymers self-assemble into highly ordered, *para*-crystalline microfibrils.[1] A typical cellulose microfibril is composed of 36 parallel cellulose chains in a *para*-crystalline, linear, hexagonal arrangement with a $\approx$10 nm diameter[1] known as type I cellulose. These microfibrils are approximately 70% crystalline. Crystalline cellulose I is stabilized by multiple in-plane hydrogen bonds linking planar cellulose chains and interplanar interactions involving predominantly van der Waals and hydrophobic interactions.[3] The stability of crystalline cellulose is evident in the relatively high temperature for decomposition onset ($\approx$310°C) and lack of an obvious melting temperature.[4] The network of interactions within and between cellulose chains poses an energy barrier to the solubilization of cellulose and makes cellulose insoluble in water.[5]

Although the cellulose in lignocellulosic biomass is a large reservoir of glucose, its release by enzymes is impeded, in-part, by the complex structure of plant cell walls that have evolved to be highly recalcitrant to digestion.[1,6] The insolubility in water aids in the formation of *para*-crystalline cellulose I microfibrils during synthesis.[1,2] The microfibrils are, in turn, encased by a complex network of hemicellulose polymers and lignin that aggregate into larger bundles and layers within the plant cell wall. This complexity restricts enzyme access to their substrate.

To make lignocellulosic biomass more digestible, pretreatments are generally required to fractionate the material into the constituent polymers.[7,8] Acids, alkali, and some organic liquids have been used to improve the digestibility of biomass.[9–13] Most likely, the high temperature and pressure of these thermochemical pretreatments cause some disruption in the nanostructure of cellulose microfibrils which is partially restored prior to digestion by water washes and in some cases drying.[9,14,15]

Cellulases, in general, act on individual cellulose chains.[1] In addition to the structural complexity of biomass, the *para*-crystalline ordering of cellulose microfibrils at the nanoscale reduces cellulase accessibility to individual cellulose chains that can be improved by pretreatments.[16,17] An example is the limited digestibility of Avicel ($\approx$ 70% crystalline cellulose) by

Trichoderma reesei Cel7A.[18] Solvents such as acetone and ethanol have been found to enhance digestibility.[6,10,19–23] Industrial processes have experimented with a variety of wash liquids including acetone, methanol, ethanol, 2-propanol, and glycols and most work has focused on the liquids that yield the highest recovery of each biomass component.[7,12,23] For example, inclusion of ethanol in the pretreatment increases glucose yields per mass of feedstock relative to other protocols.[20,23] How the ordering of the bundled cellulose chains is affected by solvent interactions that occur during pretreatments is not well understood. The X-ray diffraction used to assess the *para*-crystalline structure of cellulose provides only limited information on cellulose nanostructure and the molecular basis for its recalcitrance to digestion.[5,24]

Understanding the interactions contributing to cellulose nanostructure and the influence of solvents on these interactions is necessary to develop more highly effective cellulose pretreatments. By solubilizing cellulose in the known cellulose solvent, phosphoric acid,[25] the influence of solvents on the nanostructure of subsequent washed and precipitated cellulose was investigated. Organic wash liquids tested include those identified from the literature that enhanced the digestibility of cellulose (acetone, methanol, ethanol, 2-propanol, ethylene glycol, and water).[7,12,23] Fractal analysis of small-angle neutron scattering (SANS) of these washed materials indicated that the cellulose chains now have the properties of loosely clustered rods. Characterization of the hydrogen bonding network by Fourier transform infrared resonance (FTIR) indicated that the organic wash liquids improved the digestibility through increasing heterogeneous interpolymer hydrogen bonds and surprisingly a decrease in intrachain hydrogen bonds. This analysis led to the formulation of aqueous solvent mixtures to disrupt cellulose nanostructure.

MATERIALS AND METHODS

Washing of Cellulose
Preparation of washed cellulose followed the protocol for making phosphoric acid swollen cellulose as described by Zhang with minor modifications.[25] Avicel (PH-101; 1 g) was added to 0.6 mL water to form a slurry. 100 ml of chilled (4°C) 85 % phosphoric acid was added to dissolve the cellulose to minimize formation of cellulose phosphate esters. After 1 hour at 4°C, 400 ml of cold liquid (4°C) was added to wash the cellulose. The organic wash liquids were acetone, methanol, ethanol, 2-propanol, ethylene glycol were purchased from Sigma Aldrich and used as received. After 30 minutes, the washed cellulose was collected by centrifugation at 5,000 RPM for 10 minutes. The wash process was repeated 4 times using 250 ml of fresh liquid each time. The concentration of liquid-washed cellulose was determined by the weight of dried cellulose in 1 ml of the cellulose-liquid mixture.

Optical Characteristics
The optical characteristics of the washed cellulose suspensions were measured in two ways. First, the samples were examined visually noting opacity and settling volume. The optical density then was measured from samples in which the precipitated cellulose was well dispersed with a concentration of 5 mg/mL in 1 cm pathlength cuvettes. The optical density was monitored in a Pharmacia Biotech spectrophotometer at 600 nm over the course of 1 h and the mean of this period reported.

Digestibility of Cellulose by Enzymes
Enzyme assays were performed as described previously by Watson et al.[26] Liquid-washed phosphoric acid-swollen (PAS) cellulose was washed twice in aqueous assay buffer (20 mM PIPES [piperazine-N,N'-bis(2-ethanesulfonic acid)], 1% Instant Ocean, pH 6.5) by centrifugation at 5000 rpm for 10 min. In total, 0.1 nmol of *Saccharophagus degradans* Cel5H were used in each assay. *S. degradans* Bgl1A (0.1 nmol) was added to metabolize cellobiose to glucose.[27] All assays were conducted at 50°C. Reducing sugars were detected using the DNS (dinitrosalicylic acid) method,[28] with the average ± one standard deviation reported.

Small-Angle Neutron Scattering
SANS was performed on the 30-m NG3 beam line at the National Institute of Standards and Technology, Center for Neutron Research, Gaithersburg, MD. Each sample contained a mass fraction of 0.5% cellulose suspended in deuterated liquid obtained from Cambridge Isotope Laboratories (Andover, MA): d-acetone (99.9% D), d-ethanol (99% D), d-ethylene glycol (98% D), d-2-propanol (99% D), d-methanol (99.5% D), d-phosphoric acid (D$_3$) (85% in D$_2$O) (99% D), and d-water (99.9% D). Three instrument configurations were used to yield a range of 0.001 Å^{-1} < $q = 4\pi/\lambda\sin(\theta/2)$ < 0.474 Å^{-1} with λ equals to the neutron wavelength and θ equals to the scattering angle. Three scattering distances 13 m ($\lambda = 8$ Å), 7 m ($\lambda = 6$ Å), and 1 m ($\lambda = 6$ Å) were used for low q: 0.001 Å^{-1} < q < 0.025 Å^{-1}, intermediate q: 0.006 Å^{-1} < q < 0.077 Å^{-1}, and high q: 0.029 Å^{-1} < q < 0.474 Å^{-1}, respectively. The sample thickness was 1 mm and the sample aperture diameter was 1.27 cm. The low q configuration used a system of MgF$_2$ neutron focusing lenses that were inserted into the presample neutron flight path to yield a lower q minimum and smaller beam size on the detector.

Transmission and scattering runs from an empty and blocked beam were used for standard data correction using Igor Pro 6.11.[29] SANS data analysis was performed using a power law analysis. The scattering by each sample was divided by the contrast factor, $(\Delta\rho^2)$, to normalize for contrast variations for comparison. The intensity of scattering is a function of the differential cross-section per unit solid angle per unit volume: $d\Sigma(q)/d\Omega = I(q)$ (cm^{-1}). The average power law exponent was fit in the range of 0.0010 Å^{-1} < q < 0.15 Å^{-1} with coefficient, A and background B.[30]

$$\frac{d\sum}{d\Omega}(q) = Aq^{-\alpha} + B \qquad (1)$$

The power law exponent, α, represents the slope of the linear section of the scattering curve log(I) vs. log(q) at low to intermediate q.

Fourier Transform Infrared Resonance
Molecular characterization was performed using a Nexus 670 Fourier transform infrared spectrometer with a deuterated triglycine sulfate detector. Spectra were collected with a resolution of 4 cm^{-1} using 64 scans in the range of 400–4000 cm^{-1} and were analyzed using transmission geometry under nitrogen atmosphere. Films of washed PAS cellulose were cast by depositing 1 mg of washed PAS cellulose onto glass slides. To remove excess wash liquid, the films were held at room temperature for 16 h as described in the literature with minor modifications.[15,31–33] Then, the gelled films were removed from the glass using a razor blade.
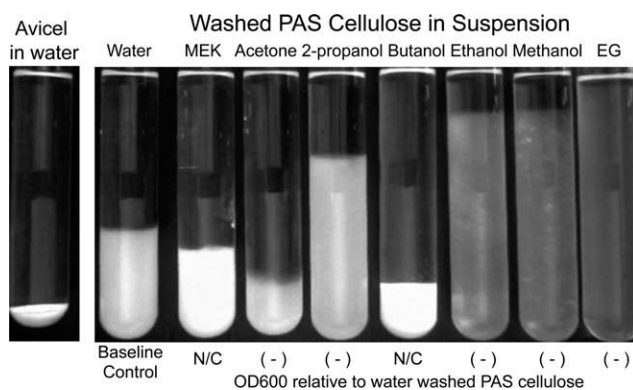
Figure 1. Effect of selected liquids on washing of phosphoric acid solubilized cellulose (PAS cellulose). Each test tube was filled with approximately 100 mg of washed PAS cellulose in a volume of approximately 30 mL and allowed to settle overnight. The OD600 evaluated the opacity of washed PAS cellulose that was well dispersed in the suspension. The OD600 was measured on the 5 mg/mL suspensions of washed material in the respective solvent and reported relative to water washed PAS cellulose as no change (N/C) or decrease in OD600 (–).

The automatic peak finder in Omnic 6.2 with a sensitivity of 100 was used to detect peak location and absorbance of peaks in the range of 970–1190 cm^{-1} and >2900 cm^{-1}. Difference spectra were processed using the subtraction function in Omnic 6.2. The peak absorbance values were analyzed from at least five unique batches of washed cellulose to calculate the instrument and experimental error (reported as one standard deviation).

X-ray Diffraction

The flash dried films of washed PAS cellulose were analyzed using a Rigaku Ultima III X-ray diffraction instrument to assess crystallinity. Avicel powder (included as a control) and cellulose films of water-washed and ethanol-washed cellulose were characterized over the range of 10–40° 2θ. The voltage was 40 kV and the current was 40 mA.

RESULTS

Influence of Organic Liquids on the Precipitation of Cellulose
Suspension of crystalline cellulose directly in the surveyed liquids at room temperature caused no substantial change in the density or morphology of cellulose over a 30+ day period as has been shown previously.[34] Instead, phosphoric acid, a known solvent for cellulose,[25] was used to solubilize cellulose (PAS cellulose) and then the selected liquids were used to wash the PAS cellulose to remove the phosphoric acid. Complete washing was confirmed by FTIR that showed the absence of peaks at wave numbers 944 and 873 cm^{-1} that would be indicative of retained phosphoric acid (data not shown). Thus, <1% of the phosphate was retained by the PAS cellulose washed with the selected organic liquids.

Some of the tested liquids had an apparent impact on the morphology of precipitated PAS cellulose as a gel-like suspension formed after the wash. The optical density of each washed PAS cellulose sample was used to estimate the impact of these washes as gels generally have lower densities, and therefore, increased transparency. Although the washed PAS cellulose

formed obvious precipitates in some organic liquids, the OD600 of washed PAS cellulose in these liquids was stable for at least 1 h after mixing. The OD600 of suspensions of PAS cellulose washed with methanol, ethanol, 2-propanol, acetone, and ethylene glycol was reduced relative to the PAS cellulose washed with the water (Figure 1 and Table I). The reduced optical densities of the washed PAS cellulose are consistent with an apparent disruption to the cellulose nanostructure. Scanning electron microscopy of the two classes of washed PAS cellulose was attempted but was uninformative (data not shown).

The apparent disruption of cellulose nanostructure after washing with the selected alcohols and glycols suggests that these materials should be more readily digestible by enzymes. *S. degradans* Cel5H, which is highly biased toward disrupted amorphous cellulose[26] and insensitive to <20% ethanol (Hutcheson, unpublished results), was used to compare the glucose yield from organic liquid and water-washed PAS cellulose. Although identical amounts of enzyme were employed and the enzyme retained indistinguishable activities during the course of the assay, ethanol-washed PAS cellulose yielded ≈ 30% more glucose than water-washed PAS cellulose (Figure 2). The glucose product was also measured from methanol- and ethylene glycol-washed PAS cellulose, but the yield was not significantly greater than that from water-washed PAS material. If the digestibility of Avicel reflects disruption of the nanostructure, the most disrupted of the washed PAS cellulose samples was the ethanol-washed PAS cellulose.

Nanoscale Properties of Organic Liquid-Washed PAS Cellulose
To evaluate the nanostructure of the washed PAS cellulose, samples were analyzed by SANS in suspensions with deuterium-substituted solvents. The relative scattering intensity at low q ($q = 0.0013$ Å^{-1}) is one indication of polymer solvation as neutron intensity decreases as solvation increases owing to a reduction in concentration fluctuations.[30] The scattering intensity at low q corresponds to scattering from cellulose bundles on the length scale of 483 nm ($d = 2\pi/q$) (Figure 3). The scattering intensity was compared for each sample relative to a control set (Table II). The control set consisted of suspensions of untreated Avicel

Table I. The Optical Density of Washed PAS Cellulose Materials

Wash liquid[a]	Optical density[b]
Starting material[c]	1.55 ± 0.0
Water (control)	2.3 ± 0.0
MEK	2.6 ± 0.4
Acetone	0.8 ± 0.0
2-Propanol	0.9 ± 0.1
Butanol	2.3 ± 0.6
Ethanol	0.8 ± 0.2
Methanol	0.6 ± 0.1
Ethylene glycol	0.4 ± 0.2

[a]The OD600 was measured from 5 mg/mL of washed PAS cellulose suspended and well dispersed in the respective solvent, [b]The starting material was 5 mg/mL Avicel suspended in water, [c]The optical density is reported as the average of triplicate samples ± one standard deviation.
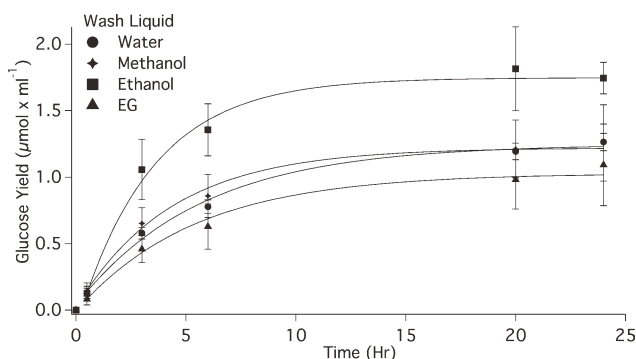
Figure 2. The digestion of washed PAS cellulose samples by *S. degradans* Cel5H. The digestion on washed PAS cellulose that had been re-equilibrated in aqueous assay buffer was compared. At each time point, the samples were centrifuged and a 50 μL aliquot of the supernatant was removed to measure the glucose concentration. The digestion did not increase significantly after 24 hr. The significance was determined from triplicate trials, and is reported as one standard deviation.

in water (negative control), water-washed PAS cellulose (conventional washing process), and cellulose solubilized in phosphoric acid (PAS cellulose, positive control). Liquid-washed PAS cellulose forming an apparent gel-like material had lower SANS intensities at low q relative to the suspension of starting material and water-washed PAS cellulose. The reduced intensity in the SANS analysis indicates that the cellulose washed in ethanol, methanol, and ethylene glycol has disrupted cellulose nanostructure relative to the acetone, 2-propanol, and water-washed material.

The liquid-washed cellulose samples exhibited characteristics of a fractal structure in the SANS analysis that could be fit using the power law [eq. (1)] to characterize the nanostructure of the
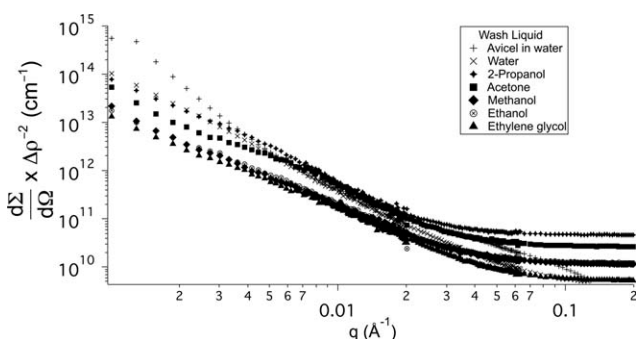

Figure 3. SANS from cellulose washed with selected liquids. Liquid-washed cellulose was resuspended in the same deuterated liquid for contrast with hydrogenated cellulose. The samples were allowed to settle for 24 h before characterization to ensure no visual phase separation. The decrease in scattering at low q relative to the starting material, and the slope of the low q region was used to compare cellulose disruption and fractal behavior. The scattering by each sample was divided by the contrast factor, $(\Delta\rho^2)$, to normalize for contrast variations enabling comparison. The instrument error was calculated for each point and was used to establish significant differences between scattering intensity of washed cellulose samples. The error bars are sufficiently small to not be shown for each sample.

washed PAS cellulose in these liquids. The power law exponent for the scattering, α, is the slope of the linear section of the scattering curve $\log(I)$ vs. $\log(q)$ at low to intermediate q $(0.0010 \text{ Å}^{-1} < q < 0.15 \text{ Å}^{-1})$ and is related to the fractal dimension of the structure.[30] The value of α obtained for the starting Avicel material was -3.56, whereas the value of α for solubilized cellulose in D_3-phosphoric acid was -1.89 (Table II). PAS cellulose washed with water exhibited an $\alpha = -2.40$ consistent with partial reformation of the cellulose nanostructure. The values of α for the gel-like PAS cellulose washed in methanol, ethanol, or ethylene glycol were -2.10, -2.17, and -2.09, respectively. In contrast, the value of α for acetone- and 2-propanol-precipitated cellulose was closer to that of the water-washed PAS material. The higher value for the power law exponent indicated methanol, ethanol, and ethylene glycol (i.e., closer to the value for PAS material) yield a more disrupted material.

FTIR Analysis of Molecular Interactions in Washed PAS Cellulose

Unique structural features of PAS cellulose washed with ethanol should be apparent by FTIR. The purpose of the molecular scale analysis is to compare the features of the ethanol-washed PAS cellulose relative to the water-washed PAS cellulose. Spectra of PAS cellulose suspended in the selected liquids were uninformative as the spectral "noise" in critical regions was masked changes as the signal-to-noise ratio was <3, which is typically the minimum value required to perform analysis of FTIR spectra.[35] Instead, flash dried films of washed PAS cellulose were analyzed by FTIR. The minimal absorbance around wavenumber 1625 cm^{-1} indicates that water was not retained in the flash

Table II. Characterization of the Nanostructure of Washed PAS Cellulose Materials by SANS

Wash liquid[a]	Neutron scattering intensity relative to starting material[b]	Power law exponent, α[c,d,e]
Avicel in water	100 ± 8.5	3.56 ± 0.02
Water	12.5 ± 0.5	2.40 ± 0.01
Acetone	5.4 ± 0.3	2.39 ± 0.01
2-Propanol	9.8 ± 0.5	2.26 ± 0.01
Ethanol	2.1 ± 0.1	2.17 ± 0.01
Ethylene glycol	1.5 ± 0.1	2.09 ± 0.01
Methanol	2.2 ± 0.1	2.10 ± 0.01
Phosphoric acid	0.7 ± 0.2	1.89 ± 0.03

[a]PAS cellulose washed with the indicated liquid was resuspended in the respective deuterated liquid. Each cellulose sample contained a mass fraction of 0.5% cellulose, [b]The scattering intensity was corrected using the contrast factor $(\Delta\rho^2)$, [c]The power law was fit by eq. (1) to the low to intermediate q region of the scattering using the SANS data analysis macro for Igor Pro 6.11[26], [d]The statistical error is reported for each power law fit, calculated in Igor Pro 6.11, corresponds to one standard deviation, [e]The power law was fit to the scattering from unique batches of cellulose to determine the standard deviation. Duplicate trials of water, methanol, and ethylene glycol washed PAS cellulose yielded a power law exponent of (2.40 ± 0.01), (2.10 ± 0.06) and (2.09 ± 0.02), respectively. Triplicate scattering trials for ethanol washed material, yielded a power law exponent of (2.17 ± 0.06).
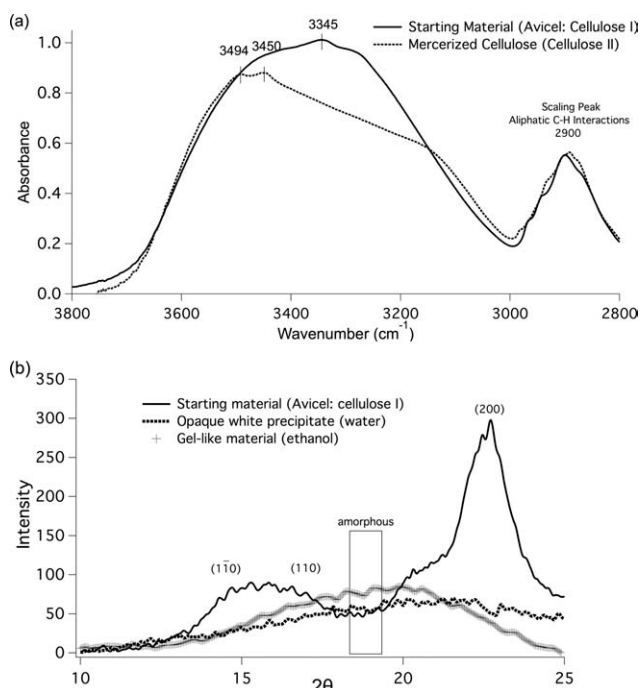
Figure 4. The impact of flash drying on the crystalline structure of cast cellulose films. (a) Native cellulose (Avicel: cellulose I) and Mercerized cellulose II were used as controls to compare both possible crystalline structures with the cellulose films. (b) The washed PAS cellulose was characterized using X-ray diffraction to determine if reformation of the crystal structure occurred. Native cellulose (Avicel: cellulose I) was used as the control to demonstrate the ability to detect crystalline peaks.

dried films of washed PAS relative to the starting material. In addition, peaks were not observed at 1046 or 1085 cm^{-1} which indicates that ethanol was separated from the flash dried films.

The impact of flash drying of the wash liquid on the cellulose crystal structure was evaluated to verify that the cellulose films were representative of the interactions in the suspensions of washed PAS cellulose. Native cellulose (Avicel : cellulose I) and crystalline cellulose II were used as controls to determine if separation of the wash liquid altered the crystal structure in the cellulose films. Peaks in FTIR analysis representing crystalline cellulose were identified at 3345 cm^{-1} (cellulose I), 3450 cm^{-1} (cellulose II), and 3494 cm^{-1} (cellulose II). These peaks were largely absent in both water- and ethanol-washed PAS cellulose [Figure 4(a)]. This suggested both samples remained in the amorphous state after separation of the wash liquid and thus were not significantly affected.

X-ray diffraction was used to confirm the amorphous character of the PAS cellulose films after separation of the wash liquid. Native cellulose in the form of Avicel : cellulose I was used as the positive control to detect peaks from crystalline cellulose. The crystallinity index of Avicel was calculated to be 73% (calculated from peak ratios[36]). The X-ray diffraction spectra for both water- and ethanol-washed PAS cellulose were in the form of broad peaks in the region of $\approx$15–25° 2θ [Figure 4(b)]. This

confirmed both PAS cellulose films were amorphous after the separation of the wash liquid.

The initial focus was on the absorbance of the glucosyl O—H groups in the region from 3000 to 3700 cm^{-1} that are associated with hydrogen bonding in cellulose. The peak at $\approx$ 2900 cm^{-1}, corresponding to aliphatic interactions from C—H bonds in the glucosyl ring structure,[37] was used to scale the spectra. A discrete peak in the spectra of water-washed PAS cellulose was observed at 3443 ± 2 cm^{-1} that could indicate an increased frequency of intrachain hydrogen bonds relative to ethanol-washed PAS cellulose [Figure 5(a)].[37,38] Only a broad peak was observed in this region in the spectra of ethanol-washed PAS cellulose.

To better characterize the differences in O—H interactions between water- and ethanol-washed PAS cellulose, a difference spectrum was calculated. The linear dependence of absorbance in this region as a function of the washed cellulose concentration indicated that Beer's Law is applicable and enables spectral subtraction. When a spectrum of water-washed PAS cellulose
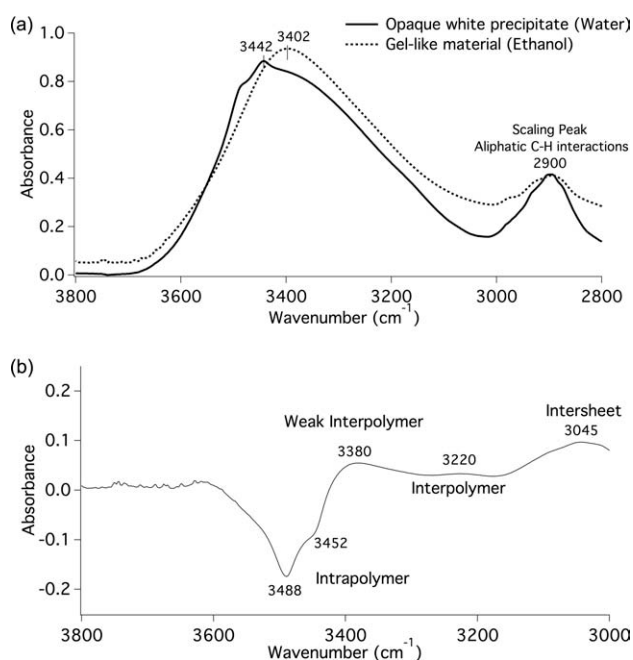

Figure 5. Characterization of the hydrogen bonding network of washed PAS cellulose. (a) The hydrogen bonding of water- and ethanol-washed PAS cellulose was characterized using FTIR. The spectra were scaled to the peak at $\approx$ 2900 cm^{-1} which represents the aliphatic C—H bonds of the glucose ring structure. The absorbance spectra were measured from cellulose films containing $\approx$ 1 mg of washed PAS cellulose with transmission geometry. Measurement of five of unique batches of washed PAS cellulose was used to determine the experimental error of the peak locations reported as one standard deviation (sufficiently small to be shown at this scale). (b) Difference spectra of water-washed PAS cellulose subtracted from ethanol washed cellulose. The difference spectra were calculated to indicate the differences in hydrogen bonding between the washed PAS cellulose samples. As the spectra of each sample were scaled prior to subtraction, a subtraction factor of 1 was used to calculate the difference. Maximum peaks indicate bonds favored in ethanol-washed PAS cellulose, whereas minimum peaks indicate bonds favored in water-washed PAS cellulose.
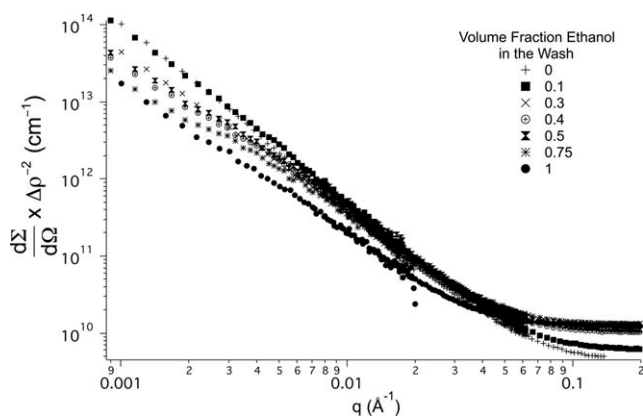
Figure 6. SANS from cellulose washed with ethanol/water mixtures. PAS cellulose washed with ethanol/water mixtures was resuspended in the same deuterated liquid for contrast with hydrogenated cellulose. The samples were allowed to settle for 24 h before characterization to ensure no visual phase separation. The scattering by each sample was divided by the contrast factor, $(\Delta\rho^2)$, to normalize for contrast variations enabling comparison. The instrument error was calculated for each point and was sufficiently small to not be shown for each sample.

was subtracted from a spectrum of ethanol-washed PAS cellulose, the difference spectrum exhibited a minimum at 3488 cm^{-1} with a shoulder at 3452 cm^{-1} consistent with greater intrachain bonding in the water-washed PAS cellulose [Figure 5(b)]. In contrast, enhanced absorbance was observed at 3380 and 3220 cm^{-1}, suggesting that interchain interactions are increased in ethanol-washed PAS cellulose relative to the water-washed material. Thus, intrachain interactions would be predicted to be more dominant in water-washed PAS cellulose, whereas interchain and intersheet interactions are likely to be more significant in the structure of ethanol-washed, gel-like PAS cellulose.

Effect of Ethanol/Water Wash Mixtures on the Cellulose Nanostructure

The apparent increased disruption to the cellulose nanostructure of PAS cellulose washed with ethanol/water mixtures was characterized to determine if mixed solvents could influence cellulose nanostructure. Cellulose nanostructure of ethanol/water mixtures was compared to PAS cellulose washed with pure liquids to determine the optimal volume fraction. SANS was used to characterize the suspensions of disrupted PAS cellulose washed with ethanol/water mixtures. The relative scattering intensity at low q is one indication of disruption as scattering intensity decreases as disruption increases owing to a reduction in concentration fluctuations (Figure 6).[30,39]

The scattering from suspensions of PAS cellulose washed with ethanol/water mixtures exhibited fractal behavior indicative of the level of clustering in the cellulose nanostructure.[30,39] To quantify the clustering of washed PAS cellulose, the average power law exponent, α, was fit in the range of 0.0030 Å^{-1} < q < 0.18 Å^{-1} using eq. (1). There was not a significant difference in the slope between the low q and the intermediate q range. The value of α was analyzed as a function of the ethanol volume fraction (V_{EtOH}) (Figure 7). The R^2 values of linear fits in the

region of V_{EtOH} =0–0.4 and 0.5 were assessed to determine at which point increasing V_{EtOH} did not further decrease the power law exponent. The highest R^2 value was 0.99 for the range of V_{EtOH} =0–0.4. The disruption of washed PAS cellulose was similar between V_{EtOH} = 0.4 ($\alpha = -2.21 \pm 0.01$) and V_{EtOH} = 1 (α of -2.17 ± 0.01) which suggests PAS cellulose forms gel-like nanostructures when V_{EtOH} = 0.4 or greater. Thus, the optimal wash mixture was V_{EtOH} = 0.4 in water.

DISCUSSION

Cellulosic materials pretreated with organic liquids have exhibited enhanced digestibility, which has been credited, in part, to improved fractionation that increases enzyme accessibility to the substrate and to a disrupted nanostructure of the constituent cellulose microfibrils.[8,18] To elucidate how these liquids might affect the cellulose nanostructure, the impact of selected organic liquids on the precipitation of cellulose was investigated. Solubilized cellulose washed with methanol, ethanol, and ethylene glycol formed significantly less aggregated, disrupted nanostructures. Wash liquids that led to the formation of opaque white precipitates, such as water, exhibited changes in the FTIR spectra in the range describing hydrogen bonding that can best be explained as more frequent intrachain interactions. This suggests that disruption of hydrogen bonds and the intrachain nanostructure are critical to the implementation of new solvent systems in pretreatment protocols.

To reduce the impact of the energy barrier to solubilization, a two-step process was employed in which cellulose was first solubilized in phosphoric acid[25] and then a second liquid was used to wash the solubilized PAS cellulose. Solvent–polymer interactions were explored in the second liquid in which retained phosphate was not apparent. When the tested liquids were used to wash PAS cellulose, two types of material were observed by the optical density and neutron scattering intensity: a gel-like suspension or an opaque white precipitate. The methanol-, ethanol-, and ethylene glycol-washed PAS cellulose materials had decreased optical densities relative to water-washed material and intensities in the SANS analysis relative to the parent material at length scales larger than $\approx$24 nm. The wash liquids water,
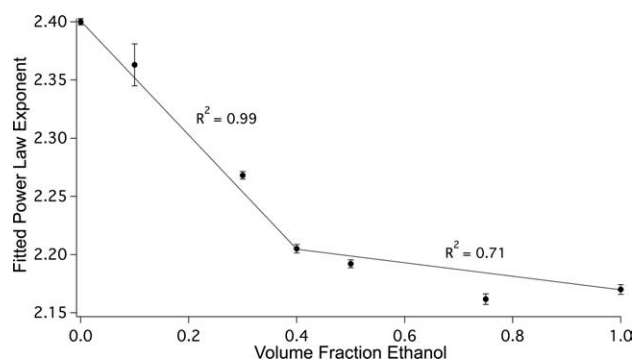

Figure 7. The power law exponent as a function of ethanol volume fraction in the wash liquid. A power law model was fit to each SANS data set to quantify the fractal behavior. The error bars represent the statistical error of each fit. The trend lines are linear fits with the R^2 value to indicate the linearity of each region.

acetone, and 2-propanol yielded relatively opaque precipitates whose physical properties suggested retention of the crystalline nanostructure. These materials exhibited poor digestion by an indicator cellulase enzyme.

The two types of washed PAS cellulose had distinct morphologies in the organic liquids. The power law exponent (α) fit to the SANS data represents the fractal dimension of the cellulose nanostructure.[30,40] The exponent α has values near -1 for isolated rigid rods, -1.66 for swollen chains, -2 for a network of rods, -3 for collapsed polymer chains, and -4 for smooth surfaces.[30] The α of Avicel, composed of 50 μm particles and suspended in water, was the average between a collapsed polymer and a smooth surface particle, and most likely represents a crystalline network of cellulose chains packed into tight bundles. Similar results were obtained for cotton linters that have not undergone significant processing (data not shown). Water-washed PAS cellulose generated by the conventional process had an α indicating some reduction in packing of cellulose bundles relative to Avicel and was similar to the published values for this material.[16,40] The value of α for PAS celluloses washed with methanol, ethanol, or ethylene glycol was closest to that of a loose network of rods in solution. The higher α of these washed materials indicates decreased ordering of the nanostructure and greater disruption relative to water-washed PAS cellulose.[17,40] Acetone- and 2-propanol-washed cellulose, in contrast, had scattering power law values similar to that of water. The increase in disruption, as indicated from the relative SANS intensity and swelling indicated by the power law analysis, indicates PAS cellulose washed with methanol, ethanol, or ethylene glycol has increased solvation, and thus, more disrupted cellulose nanostructure compared to that washed with water.

Alterations in cellulose nanostructure should be evident in hydrogen bonds of the constituent chains. Both intrachain (e.g., O3H—O5, O3H—O6, O6H—O2), and interchain (e.g., O6H—O2, O6H—O3, O2H—O2) hydrogen bonds can form in cellulose II.[38] Resolution of individual hydrogen bonds is difficult, however, owing to the disorder of the amorphous regions in cellulose and the overlapping vibrational energies of the possible hydrogen bonds within and between interacting chains. In precipitated PAS cellulose formed after washing with water, however, there was a relative increase in the predicted intrachain hydrogen bonding and a reduction in the apparent interchain hydrogen bonding as revealed by the difference spectra around the C3 hydroxyl and the effects on the C6 hydroxymethyl group. The opposite was indicated for the ethanol-washed PAS cellulose (gel-like material) in which a more heterogeneous network of interchain hydrogen bonds seemed to form.

The SANS intensity and power law analysis as well as the results from the FTIR spectroscopy gave the same result: the gel-like material formed by washing with methanol, ethanol, and ethylene glycol had disrupted nanostructures relative to the opaque white precipitate formed by washing with water. There are two possible explanations for this result: reversible crosslinking in these gel-like materials, which could be owing to the formation of interchain hydrogen bonds, would likely then inhibit the formation of intrachain hydrogen bonds; or the organic liquid through its interactions with the cellulose chains could prevent formation of interchain hydrogen bonds until the solvent is removed from the system. This argues that the precipitated cellulose obtained by washing with water is owing to other interactions such as hydrophobic and Van der Waals forces between glucosyl chains of cellulose as most are still capable of forming hydrogen bonds.

By washing PAS cellulose with ethanol/water mixtures, the ability to form hydrogen bonds could be controlled. A volume fraction of 0.4 ethanol to water was found to be optimal as evidenced by the SANS and FTIR. Both the SANS intensity at low q and the scattering power law exponent, α, indicated that after the washed PAS cellulose has undergone the gel-like transition near $V_{EtOH} = 0.4$, increasing V_{EtOH} did not further disrupt the nanostructure and was thus the most effective wash liquid mixture. The gel-like cellulose nanostructures observed in ethanol-washed cellulose were related to heterogeneous interpolymer hydrogen-bonded crosslinks. The formation of the opaque white precipitate for water-washed materials was the result of more highly ordered intrapolymer and hydroxymethyl groups in a structure similar to crystalline cellulose II. Interestingly, increased polar interactions from the water did not increase the observed disruption relative to PAS cellulose washed with pure ethanol. Even the incomplete solvation of cellulose by an organic liquid and its partial reversal by equilibration in aqueous buffer, improved the digestion of treated cellulose by enzymes. These results indicate that inclusion and retention of an organic liquid, such as ethanol, in a pretreatment leads to disrupted cellulose nanostructure and a more digestible material.

REFERENCES

1. Himmel, M. E. *Science* **2007,** *316,* 982.
2. Rubin, E. M. *Nature* **2008,** *454,* 841.
3. Jarvis, M. *Nature* **2003,** *426,* 611.
4. Kim, U. J.; Eom, S. H.; Wada, M. *Polym. Degrad. Stab.* **2010,** *95,* 778.
5. Lindman, B.; Karlstrom, G.; Stigsson, L. *J. Mol. Liq.* **2010,** *156,* 76.
6. Suvorov, M.; Kumar, R.; Zhang, H.; Hutcheson, S. *Biofuels* **2010,** *2,* 59.
7. Zhu, Z. G.; Sathitsuksanoh, N.; Vinzant, T.; Schell, D. J.; McMillan, J. D.; Zhang, Y. H. P. *Biotechnol. Bioeng.* **2009,** *103,* 715.

Applied Polymer
JOURNAL OF · SCIENCE

8. Zhang, Y. H. P.; Ding, S. Y.; Mielenz, J. R.; Cui, J. B.; Elander, R. T.; Laser, M.; Himmel, M. E.; McMillan, J. R.; Lynd, L. R. *Biotechnol. Bioeng.* **2007,** *97,* 214.

9. Mosier, N.; Wyman, C.; Dale, B.; Elander, R.; Lee, Y. Y.; Holtzapple, M.; Ladisch, M. *Bioresour. Technol.* **2005,** *96,* 673.

10. Kumar, P.; Barrett, D. M.; Delwiche, M. J.; Stroeve, P. *Ind. Eng. Chem. Res.* **2009,** *48,* 3713.

11. Lauand. M. W.; Dale, B. E. *Proc. Natl. Acad. Sci. USA* **2009,** *106,* 1368.

12. Moxley, G.; Zhu, Z. G.; Zhang, Y. H. P. *J. Agric. Food Chem.* **2008,** *56,* 7885.

13. Gupta, R.; Khasa, Y. P.; Kuhad, R. C. *Carbohydr. Polym.* **2001,** *84,* 1103.

14. Kontturi, E.; Tammelin, T.; Osterberg, M. *Chem. Soc. Rev.* **2006,** *35,* 1287.

15. Kontturi, E.; Thune, P. C.; Niemantsverdriet, J. W. *Langmuir* **2003,** *19,* 5735.

16. Pingali, S. V.; Urban, V. S.; Heller, W. T.; McGaughey, J.; O'Neill, H.; Foston, M.; Myles, D. A.; Ragauskas, A.; Evans, B. R. *Biomacromolecules* **2010,** *11,* 2329.

17. Kent, M. S.; Cheng, G.; Murton, J. K.; Carles, E. L.; Dibble, D. C.; Zendejas, F.; Rodriquez, M. A.; Tran, H.; Holmes, B.; Simmons, B. A.; Knierim, B.; Auer, M.; Banuelos, J. L.; Urquidi, J.; Hjelm, R. P. *Biomacromolecules* **2010,** *11,* 357.

18. Jeoh, T.; Ishizawa, C. I.; Davis, M. F.; Himmel, M. E.; Adney, W. S.; Johnson, D. K. *Biotechnol. Bioeng.* **2007,** *98,* 112.

19. Sathitsuksanoh, N.; Zhu, Z. G.; Templeton, N.; Rollin, J. A.; Harvey, S. P.; Zhang, Y. H. P. *Ind. Eng. Chem. Res.* **2009,** *48,* 6441.

20. Brosse, N.; Sannigrahi, P.; Ragauskas, A. *Ind. Eng. Chem. Res.* **2009,** *48,* 8328.

21. Hallac, B. B.; Sannigrahi, P.; Pu, Y.; Ray, M.; Murphy, R. J.; Ragauskas, A. *J. Ind. Eng. Chem. Res.* **2010,** *49,* 1467.

22. Sun, F. B.; Chen, H. Z. *Bioresour. Technol.* **2008,** *99,* 6156.

23. Zhao, X. B.; Cheng, K. K.; Liu, D. H. *Appl. Microbiol. Biotechnol.* **2009,** *82,* 815.

24. Park, S.; Baker, J. O.; Himmel, M. E.; Parilla, P. A.; Johnson, D. K. *Biotechnol. Biofuels* **2010,** *3,* 10.

25. Zhang, Y. H. P.; Cui, J. B.; Lynd, L. R.; Kuang, L. R. *Biomacromolecules* **2006,** *7,* 644.

26. Watson, B. J.; Zhang, H. T.; Longmire, A. G.; Moon, Y. H.; Hutcheson, S. W. *J. Bacteriol.* **2009,** *191,* 5697.

27. Zhang, H.; Moon, Y.; Watson, B.; Suvorov, M.; Santos, E.; Sinnott, C.; Hutcheson, S. *J. Ind. Microbiol. Biotechnol.* **2011,** *38,* 1117.

28. Ghose, T. K. *Pure Appl. Chem.* **1987,** *59,* 257.

29. Kline, S. R. *J. Appl. Crystallogr.* **2006,** *39,* 895.

30. Higgins, J. S.; Benoît, H. Polymers and Neutron Scattering; Clarendon Press: Oxford, **1994.**

31. Gunnars, S.; Wagberg, L.; Stuart, M. A. C. *Cellulose* **2002,** *9,* 239.

32. Kadokawa, J. I.; Murakami, M. A.; Kaneko, Y. *Carbohydr. Res.* **2008,** *343,* 769.

33. Edgar, C. D.; Gray, D. G. *Cellulose* **2003,** *10,* 299.

34. Boluk, Y. *Cellulose* **2005,** *12,* 577.

35. Smith, B. C. Fundamentals of Fourier Transform Infrared Spectroscopy; CRC Press: Boca Raton, **1996.**

36. Bansal, P.; Hall, M.; Realff, M. J.; Lee, J. H.; Bommarius, A. S. *Bioresour. Technol.* **2010,** *101,* 4461.

37. Marechal, Y.; Chanzy, H. *J. Mol. Struct.* **2000,** *523,* 183.

38. Sturcova, A.; His, I.; Wess, T. J.; Cameron, G.; Jarvis, M. C. *Biomacromolecules* **2003,** *4,* 1589.

39. Hammouda, B. Probing Nanoscale Structures: The SANS Toolbox, NIST Center for Neutron Research, **2008.**

40. Koizumi, S.; Yue, Z.; Tomita, Y.; Kondo, T.; Iwase, H.; Yamaguchi, D.; Hashimoto, T. *Eur. Phys. J. E* **2008,** *26,* 137.